ISSN1027-5495. Functional Materials, 24, No.2 (2017), p. 264-269
doi:https://doi.org/10.15407/fm24.02.264

Effect of Y addition on the microstructures and mechanical properties of Mg–Gd–Y–Sm–Zr alloys

Fu sanling[1], Li quanan[2], Chen Jun[2], Zhang Qing[2]

[1]College of Physics and Engineering; Henan University of Science and Technology, Luoyang, 471023, China
[2] School of Materials Science and Engineering; Henan University of Science and Technology, Luoyang 471023, China

Recieved December 22, 2016

The microstructure and mechanical properties of Mg–12Gd–xY–Sm–0.5Zr (x = 0, 1, 3, 5; mass%) alloys were investigated. Results showed ß'-Mg_5Gd phase composition evolution of Mg_5(Gd,Y). The tensile strength of the alloys are better the WE54 alloy at high temperatures (200–300 °C). The optimal mechanical properties of the Mg-12Gd-3Y-1Sm-0.5Zr alloy are achieved at high temperatures, and the maximum tensile strength of this alloy is 323 MPa at 250 °C. The short heat-resisting performance of Mg–Gd–Y–Sm–Zr alloys under the high temperature will provide new scientific basis for the development of heat resistant magnesium alloys.
Keywords: Y, Mg–Gd–Sm–Zr alloy, microstructure, tensile property.

Исследованы микроструктура и механические свойства сплавов Mg-12Gd-xY-Sm-0.5Zr (*x* = 0, 1, 5,%). Результаты показали, что фазовый состав ß'-Mg_5Gd эволюционирует в Mg_5 (Gd, Y). Прочность на растяжение этих сплавов лучше сплава WE54 при высоких температурах (200-300 °C). Оптимальные механические свойства сплава Mg-12Gd-3Y-1Sm-0.5Zr достигаются при высоких температурах, а максимальная прочность на растяжение этого сплава составляет 323 МПа при 250 °C. Жаростойкие сплавы Mg-Gd-Y-Sm-Zr при высокой температуре станут новой научной основой для разработки термостойких магниевых сплавов.

Вплив додавання Y на мікроструктуру і механічні властивості сплавів Mg-Gd-Y-Sm-Zr. *Фу Санлин, Ли Цюанан, Чэнь Цзюнь, Чжан Цин*

Досліджено мікроструктура і механічні властивості сплавів Mg-12Gd-xY-Sm-0.5Zr (*x* = 0, 1, 5,%). Результати показали, що фазовий склад ß'-Mg_5Gd еволюціонує в Mg5 (Gd, Y). Міцність на розтяг сплавів краще сплаву WE54 при високих температурах (200-300 °C). Оптимальні механічні властивості сплаву Mg-12Gd-3Y-1Sm-0.5Zr досягаються при високих температурах, а максимальна міцність на розтягнення цього сплаву становить 323 МПа при 250 °C. Жаростойкие сплави Mg-Gd-Y-Sm-Zr при високій температурі стануть новою науковою основою для розробки термостійких магнієвих сплавів.

1. Introduction

Energy saving and environment protection have become important concerns worldwide. Consequently, increasing efforts have been exerted to develop lightweight Mg-based structural materials that feature low density and high specific stiffness. However, the low mechanical properties and poor corrosive resistance of Mg alloys limit their applications. Hence, other alloying elements are added to improve the mechanical and anticorrosive properties of Mg alloys. Rare earth (RE) elements are effective alloying elements for Mg alloys [1,2]. Mg alloys

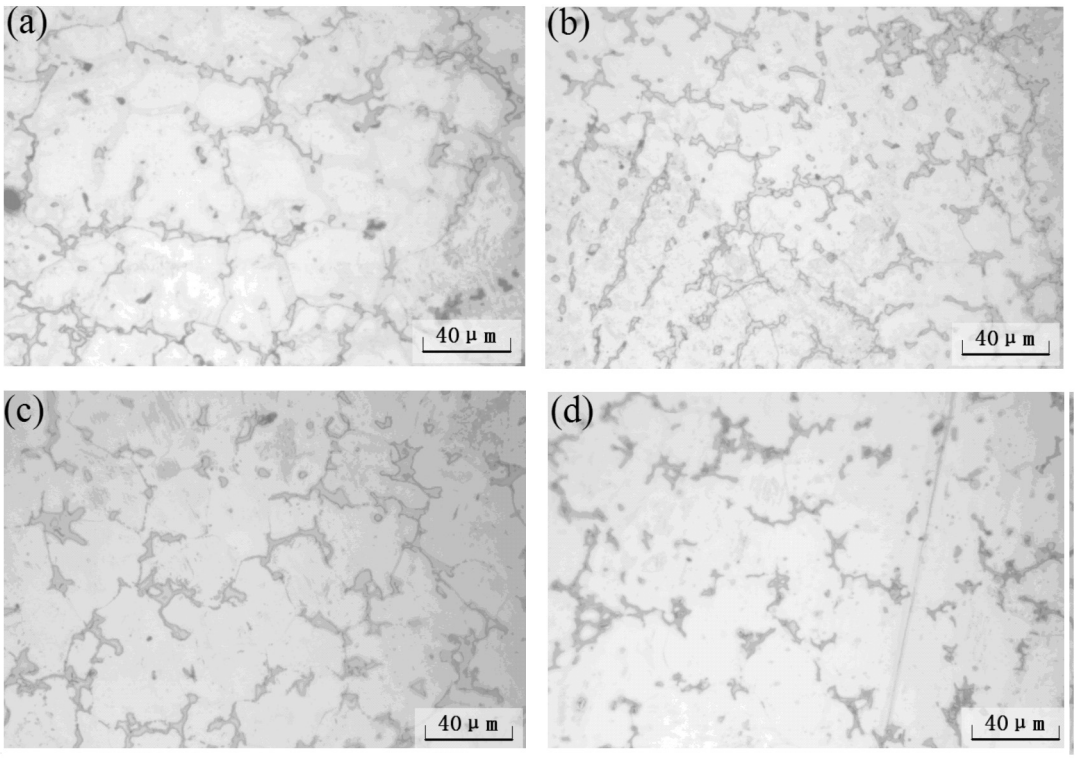

Fig. 1. Optical micrographs of as-cast Mg-12Gd-xY-1Sm-0.5Zr alloys: (a) x=0, (b) x=1, (c) x=3, and (d) x=5

containing RE elements offer favorable mechanical properties, such as high anticorrosive properties and good cast ability, particularly at temperatures exceeding 200 °C. These alloys exhibit considerable potential applications in the automotive industry. Therefore, recent studies have focused on the development of novel Mg–RE (Gd, Nd, Er, and Y) alloys[3–7]. The solubility of Gd in Mg can reach 23.5% (mass fraction) at a eutectic temperature of 548 °C, but this value decreases to 3.82% (mass fraction) as the temperature decreases to 200 °C. Changes in solubility significantly affect the mechanical properties of alloys through solution strengthening and precipitation hardening [8,9]. Y and Sm are partly replaced by Gd because of their higher cost performance than Gd, and Y can promote the precipitation of Mg_5Gd phase and combined with Mg-Gd phase to form a better performance of $Mg_5(Gd,Y)$ phase. However, contributions concerning the microstructure evolution and mechanical properties of Mg–Gd–Sm–Zr alloys are rarely reported. Sm is a fairly effective and relatively economic RE alloying element. The strength of Mg–Gd–Y alloys increases with the addition of 1% Sm [10]. Despite the efficient alloying strengthening effect of Sm, few studies reported on the addition of Sm. In the present study, the microstructure and tensile properties of Mg–Gd–Sm–Zr-based alloys with Y addition were studied.

2. Materials and methods

Alloys with a nominal composition of Mg–12Gd–xY–1Sm–0.5Zr (x=0, 1, 3, 5; mass%) were prepared from Mg (99.98% pure), Mg–30Gd (mass%), Mg–25Y (mass%), Mg–30Sm (mass%), and Mg–25Zr (mass%) master alloys in a corundum crucible under a mixed atmosphere of CO_2 and SF_6 Subsequently, these alloys were poured into an electric resistance furnace. The melted mixture was poured into a steel mold and cooled down at room temperature. The samples were machined from the casting, covered with MgO powder before being heated for solution treatment at 525 °C for 6 h, and then quenched in water. Artificial aging treatments were performed at 225 °C for 10 h. Tensile test with a tensile speed of 1 mm/min was tested by Shimadzu AUTOGRAPH (AG-I 250kN, Japan) at room temperature, 200 °C, 250 °C, and 300 °C. High-temperature tensile was heat preserved for 5 min under the corresponding temperature. The microstructures, fracture morphology, and alloy composition were observed and analyzed via optical microscopy, scanning electron microscopy (SEM), energy dispersive spectrometry (EDS), and transmission electron microscopy (TEM). Specimens for TEM were prepared via electrolytic double-jet thinning in a solution of 30% (volume fraction) HNO_3 in methanol. Alloy phase analysis

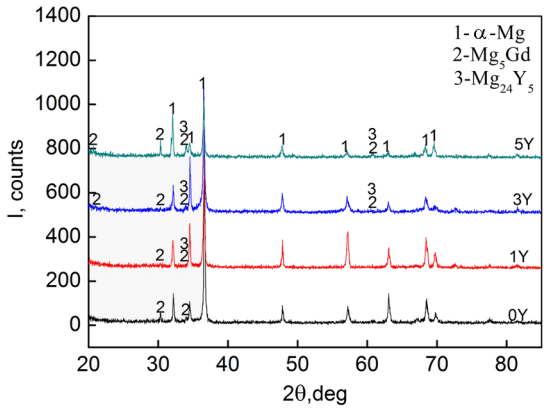

Fig. 2. X-ray diffraction patterns of solid solution-treated Mg–12Gd–xY–1Sm–0.5Zr alloys.

was also carried out through X-ray diffraction (XRD). Grain size was determined from a large number of non-overlapping measurements by using a linear intercept method.

3. Results and discussion

The microstructures of the as-cast alloys are shown in Fig. (1). As shown in the micrograph, the microstructures of all the as-cast alloys are composed of α-Mg matrix and coarse dendrite.

When the alloy is without Y, the dendrite shape is connected together and coarse, and the middle is surrounded by a white α-Mg matrix area. Thus, the cast alloy grain without Y can be relatively large compared with other samples. Figs. (1b–1d) show the microstructures of the as-cast alloys added with Y. The secondary phases, which are intensive dendrites, have intermittent shape distribution, and the middle region surrounded by a white α-Mg matrix area is relatively small. Moreover, the grain size of all the as-cast alloys decreases with the addition of Y. The alloy sizes are 32, 20, 29, and 30 μm, which are shown in Fig. (1a), (1b), (1c), and (1d), respectively. The alloys display the lowest grain size when the Y content is 1%.

The XRD patterns of the alloys homogenized at 225 °C for 10 h analysis shown in Fig. (2). As shown in the diagram, the XRD patterns of all experimental alloys are mainly composed of α-Mg, Mg_5Gd, and $Mg_{24}Y_5$ characteristic absorption peaks. The alloys added with Y contain the $Mg_{24}Y_5$ phase, and the $Mg_{24}Y_5$ characteristic absorption peak becomes apparent with increasing Y. The Gd and Y atoms in the ß' phase can replace each other because of their similar atomic radii (0.178 and 0.182 nm, respectively) and electronegativities (1.20 and 1.22, respectively) [10]. Such replacement can be formed using the bottom heart orthogonal structure of Mg_5(Gd, Y), thus the ß' phase composition evolution of Mg_5(Gd, Y) and ß' in Ref. [12] The characteristic diffraction peaks of $Mg_{24}Y_5$, Mg_5Gd, and Mg_5(Gd, Y) are overlapping and almost unable to separate. Not marked in the picture with the characteristics of Sm diffraction peak due to less Sm elements are added.

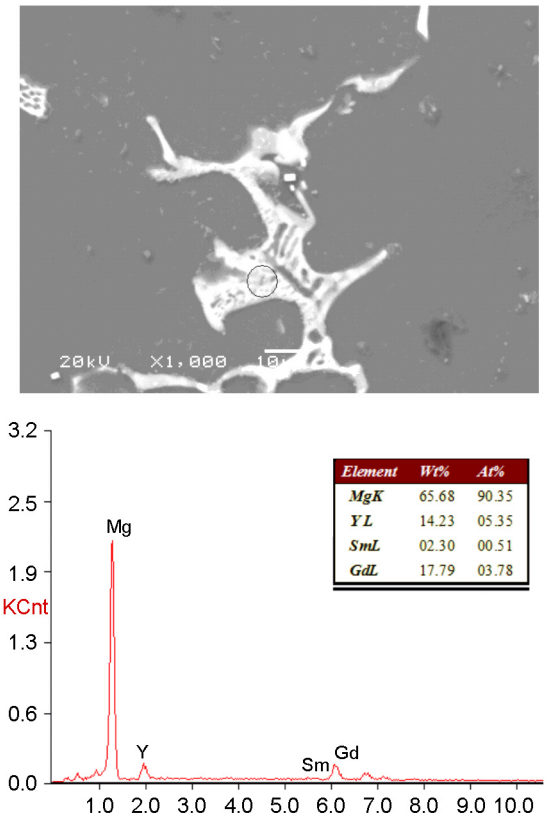

Fig. 3. Scanning electron micrograph and energy dispersive spectral analysis of the microstructure of the Mg–12Gd–3Y–1Sm–0.5Zr alloy.

The SEM and corresponding EDS results on the morphology of the Mg–12Gd–xY–1Sm–0.5Zr alloys are shown in Fig. (3), the precipitation phase of the experimental alloy comprises discontinuous dendrites that are distributed along the grain boundaries. In order to determine the distribution of elements, EDS was carried out in boundary intermittent dendrites, the results indicate which is enriched in Mg, Gd, Y, and Sm. The atomic ratios of Y and Gd in the two types of compounds are 5.35 and 3.78, respectively. The EDS results further verify that the addition of Y to the Mg–Gd–Sm–Zr alloy causes the formation of the $Mg_{24}Y_5$ phase. Previous investigations on the effects of RE on Mg alloys reported that adding Y to Mg–Gd–Sm–Zr alloys causes the formation of a new $Mg_{24}Y_5$ phase. The possibility of compound formation between Mg and Y atoms can be estimated using the electronegativity differences. XRD analysis shows that secondary phases can be identified as an intermittent dendrite compound composed of the Mg_5Gd and $Mg_{24}Y_5$ phases.

The TEM images of aged Mg–12Gd–3Y–1Sm–0.5Zr alloy are shown in Fig. (4), bright-field (BF) image electron beam and corresponding selected area electron diffraction (SAED) pattern. It is known that the alloy composed of white α-Mg matrix and black granular precipitated phase in the Fig. (4a). There are three ß' phase small diffraction spots evenly spaced distribution in between the α-Mg(010) from the analysis of rectangular box corresponding SAED, and the ß' phase located in 1/4 (010) α, 1/2 (010) α, 3/4 (010) α successively .

The ß' phase is the main secondary phase. Fig. (4a) shows the direction of the arrow using the black strip precipitates, and the size is below 20-40 nm. Fig. (4b) shows the corresponding SAED and precipitation of high-resolution TEM and corresponding Fourier transformation diagram. The precipitated phase can be determined for the nanoscale precipitated ß' phase with mole stripe, the results with the corresponding Fig. (4b) is consistent with FFT, and the experiment indicates that the phase can effectively strengthen the alloy.

The mechanical properties of the Mg–12Gd–xY–1Sm–0.5Zr alloys are shown in Fig. (5). The best tensile strength and yield strength are obtained upon the addition of 3% Y at room temperature, but the elongation decreases with increasing Y content. Alloy tensile strength is reduced after the first rise with the increase in stretching temperature. The alloy added with 3% Y displays optimal mechanical properties at a high temperature. This result indicates that a moderate amount of Y addition is crucial to improve the heat-resistant properties of alloys. The tensile strength of the Mg–Gd–Y–Sm–Zr alloys initially increases, decreases, and then peaks at 250 °C with increasing test temperature. The yield strength decreases with increasing stretching temperature, but the elongation increases with increasing test temperature.

In the commercial department of Mg–RE heat-resistant Mg alloys, the WE54 alloy exhibits the most suitable high-temperature mechanical properties; its T6 state at room-temperature mechanical properties is as follows: σ_b=280 MPa, $\sigma_{0.2}$=205 MPa, and δ=4%[13]. The mechanical properties of the Mg–Gd–Y–Sm–Zr alloys are close to those of the WE54 alloy at room temperature but are better at high temperatures (200–300°C). The optimal mechanical properties of the Mg-12Gd-3Y-1Sm-0.5Zr alloy are obtained at high temperatures, and the maximum tensile strength is 323 MPa at 250 °C. The Mg-12Gd-3Y-1Sm-0.5Zr alloy also exhibits favorable mechanical properties at a high temperature of 300 °C, and the tensile

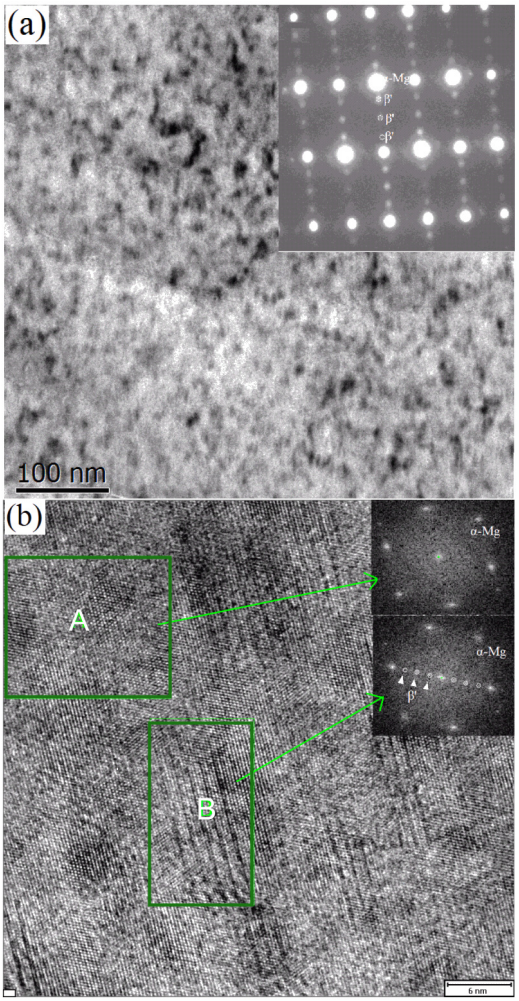

Fig. 4. Transmission electron micrographs recorded from the Mg–12Gd–3Y–1Sm–0.5Zr alloy after T6 treatment. (a) bright-field image and the illustrations for the corresponding SAED; (b) Corresponding HRTEM image and FFT patterns obtained from areas A and B in (b), respectively.

strength, yield strength, and elongation of this alloy are 293 MPa, 203 MPa, and 6.45%, respectively.

As is known to all, the design features of mechanical property in metal materials is that the bonding force between the metal atoms reduced with the increase of temperature, and the tensile strength decreased and the elongation increased with the increase of stretching temperature. Tensile strength of Mg–12Gd–xY–1Sm–0.5Zr series magnesium alloys appeared abnormal phenomenon, and the tensile strength did not reduce with increasing stretching temperature, but increased significantly, at room temperature to 250 °C in this experiment. The short heat-resisting performance of Mg–12Gd–xY–1Sm–0.5Zr series magnesium alloys under the high temperature will provide

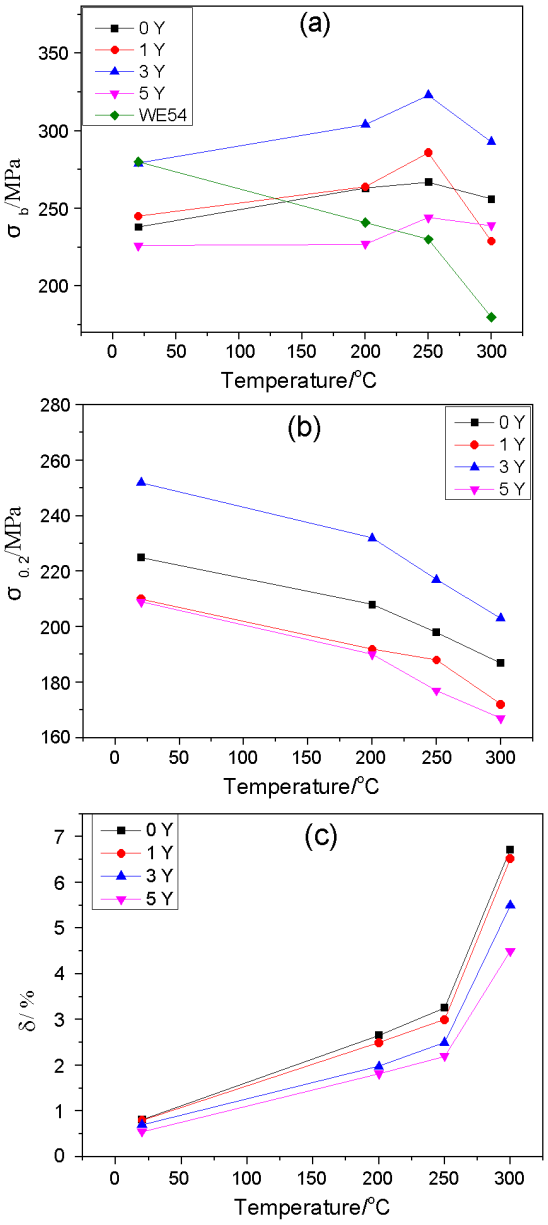

Fig. 5. The mechanical properties of the Mg–12Gd–xY–1Sm–0.5Zr alloys. (a) – tensile strength; (b) – yield strength; (c) – elongation

experimental basis in the application of missile hull, and which will provide new scientific basis for the development of heat resistant magnesium alloys.

In this study, Y improves the mechanical properties of the Mg–Gd–Y–Sm–Zr alloys in addition to achieve strengthening of grain refinement, and due to Gd in the Mg balance has a high solubility. With the decrease in temperature, the solubility of exponential decreases quickly, and precipitation forms an ideal reinforcement system. Mg_5Gd is a product of alloy during solidification, with a punctate or dendritic distribution on the grain boundaries or intermediate dendrite spacing. In addition, the $Mg_5(Gd,Y)$ phase has high-temperature stability in high phase. These phases are distributed in the α-Mg matrix, and the equivalent of hard particles embedded in the matrix of some irregular punctate or branched during tensile tests can hinder the movement of dislocations and grain deformation. Consequently, the strength of the Mg–Gd–Y–Sm–Zr alloys is improved.

The metal-mold casting conditions are as follows: the cooling rate is higher than the balance of cooling required for speed, which belongs to the non-equilibrium solidification. Furthermore, at a high-temperature solid solution on the base of the α-Mg part of the Gd, Y is preserved at room temperature, and a supersaturated solid solution is formed because the difference in the atomic radius of Mg is large. The solution on the base of α-Mg results in serious distortion of the lattice and solid solution strengthening effect, thereby improving the mechanical properties of the alloy.

4. Conclusions

Y has properties similar to those of other RE elements. These elements function in the purification of Mg solution, hydrogen removal, and grain refinement. Moreover, the atomic radius of Y is similar to that of Mg, and the Y in the solid solubility of Mg is large. Solid solubility also decreases with rapidly decreasing temperature. Therefore, the addition of Y in Mg can result in the strengthening of fine grains, solid solution, and precipitation. Thus, the addition of Y in Mg can effectively improve the microstructure and mechanical properties of the alloy. In this study, the specific roles of Y in the Mg–Gd–Y–Sm–Zr alloy are discussed and summarized as follows:

(1) Y plays an important role in refining the grain of the Mg–12Gd–xY–1Sm–0.5Zr alloy. When the Y content is 1%, the cast alloy exhibits the most obvious grain refinement;

(2) The mechanical properties of the Mg–Gd–Y–Sm–Zr alloys are similar to those of the WE54 alloy at room temperature but better at high temperatures (200–300 °C). The optimal mechanical properties of the Mg-12Gd-3Y-1Sm-0.5Zr alloy are obtained at high temperatures, and the maximum tensile strength of this alloy is 323 MPa at 250 °C. The Mg-12Gd-3Y-1Sm-0.5Zr alloy also demonstrates favorable mechanical properties at a high temperature of 300 °C, and the tensile strength, yield strength,

elongation of this alloy are 293 MPa, 203 MPa, and 6.45% respectively;

(3) Mg–Gd–Y–Sm–Zr alloys mainly via strengthening of grain refinement, solid solution and secondary phase.

Acknowledgements

This work was supported by National Natural Science Foundation of China (51571084, 51171059), Scientific and Technological Project of Henan Province (Grant No. 152102210072), the Basic and Frontier Technologies Research Plan of Henan Province (102300410018), and the Program for Innovative Research Team (in Science and Technology) in the University of Henan Province (2012IRTSTHN008).

References

1. B.**L.Mordike and T. Ebert,** *Mat. Sci. Eng A*, . **302**,. 37, 2001.
2. X.**Y. Xia, A.A. Luo, D.S. Stone,** *J. Alloy.Comp.*, **649**, 649, 2015.
3. S. Zhang, W.C. Liu, X.Y. Gu, C. Lu, et al, *J. Alloy.Comp.*.**557,** 91, 2013.
4. K.Y. Zheng, J. Dong, X.Q. Zeng W.J. Ding, *Mat. Charact.*, **59**, 857, 2008.
5. X. Xia, K. Zhang, X. Li, M. Ma, Y. Li. *Mat.Design*, **44**, 521, 2013.
6. Z.**H. Wang, W.B. Du, X.D. Wang, et al** *Trans. Nonferr. Metals Soc. China*, **23**, 593, 2013.
7. **Y.B. Hu, J. Deng, C. Zhao, et al,** *Trans.Nonferr. Metals Soc. China*, **21**, 732, 2011.
8. **Q.M. Peng, N. Ma, H. Li,** *J. Rare Earths*, **30**, 1064, 2012.
9. **Y. Gao, H. Liu, R. Shi, et al,** *Acta Mat.*, **61**, 453, 2013.
10. **J.L. Wang, L.D. Wang, Y.M. Wu,,** *Mat. Sci.Eng. A*, **528**, **4115, 2011.**
11. T. **Honma, T. Ohkubo, K. Hono, S. Kamado,** *Mat. Sci. Eng.: A*, **395**, 301, **2005.**
12. Z. Yang, J.P. Li, Y.X. Wu, Z.L. Yang, *Foundry*, **62**, 545, 2013.
13. Z.Y. Zhang, L.M. Peng, X.Q. Zeng, et al *Mat. Charact.*, **60**, 555, 2009.